Published in final edited form as:

Science. 2016 March 25; 351(6280): 1458–1463. doi:10.1126/science.aad9195.

HIV-1 broadly neutralizing antibody precursor B cells revealed by germline-targeting immunogen

Joseph G. Jardine[1,2,3,*], **Daniel W. Kulp**[1,2,3,*], **Colin Havenar-Daughton**[3,4,*], **Anita Sarkar**[2,3,5,*], **Bryan Briney**[1,2,3,*], **Devin Sok**[1,2,3,*], **Fabian Sesterhenn**[1,#], **June Ereño-Orbea**[6], **Oleksandr Kalyuzhniy**[1,2,3], **Isaiah Deresa**[3,4], **Xiaozhen Hu**[1,3], **Skye Spencer**[1,3], **Meaghan Jones**[1,3], **Erik Georgeson**[1,3], **Yumiko Adachi**[1,2,3], **Michael Kubitz**[1,2,3], **Allan C. deCamp**[7], **Jean-Philippe Julien**[2,3,5,6,8], **Ian A. Wilson**[2,3,5,9], **Dennis R. Burton**[1,2,3,10], **Shane Crotty**[3,4,11,†], and **William R. Schief**[1,2,3,10,†]

[1]Department of Immunology and Microbial Science, The Scripps Research Institute, La Jolla, CA 92037, USA

[2]IAVI Neutralizing Antibody Center, The Scripps Research Institute, La Jolla, CA 92037, USA

[3]Center for HIV/AIDS Vaccine Immunology and Immunogen Discovery, The Scripps Research Institute, La Jolla, CA 92037, USA

[4]Division of Vaccine Discovery, La Jolla Institute for Allergy and Immunology, La Jolla, CA 92037, USA

[5]Department of Integrative Structural and Computational Biology, The Scripps Research Institute, La Jolla, CA 92037, USA

[6]Program in Molecular Structure and Function, The Hospital for Sick Children Research Institute, Toronto, Ontario, M5G 0A4, Canada

[7]Vaccine and Infectious Disease Division, Statistical Center for HIV/AIDS Research and Prevention (SCHARP), Fred Hutchinson Cancer Research Center, Seattle, WA 98109

[8]Departments of Biochemistry and Immunology, University of Toronto, Toronto, Ontario, M5S 1A8, Canada

[9]Skaggs Institute for Chemical Biology, The Scripps Research Institute, La Jolla, CA 92037, USA

[10]Ragon Institute of MGH, MIT, and Harvard, Cambridge, MA 02129, USA

[11]Division of Infectious Diseases, Department of Medicine, UCSD School of Medicine, La Jolla, CA

Abstract

Induction of broadly neutralizing antibodies (bnAbs) is a major HIV vaccine goal. Germline-targeting immunogens aim to initiate bnAb induction by activating bnAb germline precursor B

[†]To whom correspondence should be addressed: ; Email: schief@scripps.edu or ; Email: shane@lji.org.
[#]Current address: Institute of Bioengineering, École Polytechnique Fédérale de Lausanne, CH-1015 Lausanne, Switzerland
[*]These authors contributed equally to the work.

Supplementary Content: Materials and Methods, figs. S1 to S14, tables S1 to S7, references 28–41.

cells. Critical unmet challenges are to determine whether bnAb precursor naïve B cells bind germline-targeting immunogens and occur at sufficient frequency in humans for reliable vaccine responses. We employed deep mutational scanning and multi-target optimization to develop a germline-targeting immunogen (eOD-GT8) for diverse VRC01-class bnAbs. We then used the immunogen to isolate VRC01-class precursor naïve B cells from HIV-uninfected donors. Frequencies of true VRC01-class precursors, their structures, and their eOD-GT8 affinities support this immunogen as a candidate human vaccine prime. These methods could be applied to germline targeting for other classes of HIV bnAbs and for Abs to other pathogens.

Development of an HIV vaccine is a global health priority. Recent discoveries of potent broadly neutralizing antibodies (bnAbs) that bind to relatively conserved epitopes on the HIV Env glycoprotein trimer and protect against challenge in animal models have reinvigorated vaccine design efforts to induce bnAbs (1). However, bnAbs have not been elicited in standard animal models or humans.

Germline targeting, a vaccine priming strategy to initiate the affinity maturation of select germline-precursor B cells, has promise to initiate bnAb induction. The goals for a germline-targeting prime are to activate B cell precursors with bnAb potential, select productive (bnAb-like) somatic mutations, and generate an expanded population of memory B cells that can be boosted and matured subsequently to shepherd the response further toward bnAb development (2, 3). For a few HIV bnAbs, next generation sequencing of antibody populations during bnAb development in infected individuals has allowed bioinformatic inference of likely human germline precursors (4, 5). For most bnAbs, however, true human precursors are not known but are usually approximated by ‘germline-reverted’ antibodies that utilize inferred germline V and J genes and retain mature complementarity determining region 3 (CDR3) loops. Because CDR3 loops typically play a major role in antibody affinity and specificity, germline-reverted bnAbs are not known to be reliable proxies for true germline precursors.

VRC01-class bnAbs are an important test case for germline-targeting, because they are among the most broad and potent of HIV bnAbs, and their germline-reverted forms show no detectable affinity for HIV Env glycoproteins (6–10). Knock-in mice transgenic for a germline-reverted VRC01-class heavy chain responded to immunization with the germline-targeting eOD-GT8 60-subunit self-assembling nanoparticle (60mer) but not with native-like Env trimers, providing proof-of-principle that germline-targeting immunogens can initiate a VRC01-class response if well-matched B cells are present and competing B cells are strongly reduced in frequency (2, 3). Here we address further critical knowledge gaps for development of this, or any, germline-targeting immunogen as a human vaccine: Do the targeted bnAb precursors exist in humans? What is the frequency and person-to-person variation of germline-targeting-immunogen-specific bnAb precursors? Can the germline-targeting immunogen bind the targeted human bnAb precursors in competition with other B cells in the fully complex human B cell repertoire? We examined these questions by developing new ex vivo approaches and protein design methods.

When we employed the VRC01-class germline-targeting immunogen eOD-GT6 (9) as bait to screen human naïve B cells using a two phase multiple-validation methodology ((11) and

fig. S1), we failed to isolate VRC01-class B cells. We did, however, isolate non-VRC01-class naïve B cells with Ab affinities as low as 120 μM for eOD-GT6 (fig. S1). We therefore set out to develop an improved variant of eOD-GT6 with higher affinity and breadth for germline-reverted VRC01-class Abs, hypothesizing that such improvements might translate into improved affinity for diverse true VRC01-class precursor Abs.

To improve on eOD-GT6, we utilized yeast display library screening coupled with next generation sequencing (12). We screened a library of every point mutation at the 58 eOD:Ab interface positions on eOD-GT7, a slightly improved version of eOD-GT6 (11), against each of 29 VRC01-class Abs (18 germline-reverted and 11 mature bnAbs). By measuring binding enrichments for each mutation and antibody (Fig. 1A and fig. S2), we identified 12 positions in eOD-GT7 at which one or more mutations were favorable (at least 2-fold enriched) for binding to the majority (at least 10 of 18) of germline-reverted bnAbs and another 4 positions at which one or more mutations were at least 1.25-fold enriched for binding to the vast majority (at least 17 of 18) of germline-reverted bnAbs (Fig. 1B). To identify combinations of mutations predicted to confer the greatest binding cross-reactivity, we then created a library encompassing all combinations of a filtered set of the favorable mutations at those 16 positions (13) (Fig. 1C). Upon screening this combinatorial library against the panel of 29 VRC01-class Abs, we identified a sequence, eOD-GT8, predicted to have optimal breadth against the entire panel (Fig. 1C, fig. S3–4 and table S1).

Compared to eOD-GT6, eOD-GT8 demonstrated superior affinity and breadth of binding to germline-reverted Abs (Fig. 1D and table S2). eOD-GT8 bound to all germline-reverted Abs in the panel, whereas eOD-GT6 bound to only 8 of 14 Abs with K_Ds < 100 μM. For those eight germline-reverted Abs, eOD-GT8 had a 2,100-fold higher geometric mean affinity compared to eOD-GT6. eOD-GT8 also had 3-fold improved affinity for VRC01-class bnAbs. The tightest eOD-GT8 binding detected was for germline-reverted PGV20, with a K_D of 508 fM (234–943 fM 95% CI) (Fig. 1D, fig. S5), a 5,900 fold improvement over eOD-GT6 (K_D = 3 nM) and a 33 million fold improvement over the original eOD construct, eOD Base (K_D = 17 μM (9)), a remarkable affinity improvement for a protein-protein interface.

To examine whether VRC01-class precursors targeted by eOD-GT8 exist in humans, we performed epitope-specific B cell sorting from a pool of peripheral blood mononuclear cells (PBMCs) from healthy, HIV-seronegative donors. Epitope-specific B cells bound tetramers of eOD-GT8 but not tetramers of eOD-GT8-KO, a variant of eOD-GT8 with mutations abrogating binding by VRC01-class germline-reverted Abs. After sequencing immunoglobulin genes from single sorted cells, we searched for VRC01-class antibody sequences—i.e. those with a heavy chain that utilized VH1-2 alleles *02, *03 or *04 and a light chain with a 5-amino acid (aa) CDR3 (9, 14). After sorting 2.4 million $IgM^{(+)}/IgG^{(-)}/CD19^{(+)}$ B cells pooled from 9 donors, we recovered a single $GT8^{(+)}/GT8\text{-}KO^{(-)}$ Ab that qualified as a VRC01-class precursor. This Ab, VRC01c-HuGL1, bound to eOD-GT8 with a K_D of 22 μM and had no detectable affinity for eOD-GT8-KO (fig. S6).

To assess both the percentage of people who possess VRC01-class germline precursor B cells and the frequency of VRC01-class germline precursor B cells within a given donor, we

screened naïve B cells from 15 healthy, HIV-seronegative donors individually rather than pooled. For 7 of 15 samples, we used the two phase multiple-validation methodology that first assesses specificity by probe binding in flow cytometry and then confirms specificity and lack of polyreactivity by single cell secreted IgM (fig. S7); for 8 subsequent donors, we relied on sorting specificity alone. To improve cell sorting sensitivity, B cells were required to simultaneously bind two eOD-GT8 probes multimerized differently (trimer, 'tri'; and streptavidin tetramers, 'SA') and not bind eOD-GT8-KO-SA (Fig. 2A and fig. S7). For the 15 donors, the mean frequency of eOD-GT8$^{(tri+/SA+)}$ B cells among 61.6 million naïve B cells sorted was 0.0056% (Fig. 2B). Strikingly, a vast majority (84% ± 14%) of these eOD-GT8$^{(tri+/SA+)}$ B cells did not bind eOD-GT8-KO-SA (Fig. 2C), suggesting that naïve B cell reactivity to eOD-GT8 is highly focused to the CD4 binding site (CD4bs) (15).

Paired heavy and kappa light chain sequences were recovered from 173 eOD-GT8$^{(tri+/SA+)}$/eOD-GT8-KO$^{(-)}$ B cells. All sequences were essentially germline, confirming the naïve B cell sorts. Half (50%) of these B cells were VH1-2, whereas only 4% of control B cells from reference (16) were VH1-2 (X^2 = 29.9, p < 0.0001; Fig. 2D and fig. S8). Among these 87 VH1-2$^+$ B cells, 26 had a light chain CDR3 (L-CDR3) length of 5 aa, an 85-fold enrichment compared to control B cells (X^2 = 32.6, p < 0.0001; Fig. 2E). Twenty-five of the 26 used the VH1-2*02 allele and one used VH1-2*04 (table S3), thus 15% (=26/173) of GT8$^{(tri+/SA+)}$/eOD-GT8-KO$^{(-)}$ B cells were VRC01-class. In total, we identified 27 independent VRC01-class naïve B cells, including VRC01c-HuGL1.

In addition to the VH1-2 alleles and critical 5-aa L-CDR3, VRC01-class bnAbs possess several additional defining features, including a consensus L-CDR3 of QQYEF. The majority of VRC01-class precursors we isolated contained a QQYxx partial VRC01-class consensus motif, significantly enriched compared to control B cells (67% vs 11%; χ^2 = 8.2, p < 0.0001; Fig. 2F). Furthermore, 11% contained a QQYEx L-CDR3 motif (vs 1.5% of control B cells), one mutation away from a perfect mature VRC01-class L-CDR3 (Fig. 2F). In addition, the L-CDR1 loop is under strong selective pressure during VRC01-class bnAb affinity maturation to minimize clashes with gp120 (6, 17). VRC01-class bnAb L-CDR1 loops generally become very short (2–6 aa) through deletion, or retain a germline length of 6 aa and add flexible glycines (17). Of the 27 VRC01-class precursors isolated by eOD-GT8, 23 used V_k genes containing L-CDR1 loops of 6–7 aa (Fig. 2G), thus confirming potential to develop into VRC01-class bnAbs. Indeed, 17 of the VRC01-class naïve B cells had V_k genes utilized in known VRC01-class bnAbs (Fig. 2H). At least 24 of the VRC01-class precursors had H-CDR3 lengths of 10–19 aa (Fig. 2I)(18), consistent with known VRC01-class bnAb lengths of 10–19 aa. Thus, not only are the eOD-GT8 isolated naïve B cells highly enriched for VRC01-class core characteristics of VH1-02 and a 5-aa L-CDR3, they possess further refined sequence attributes of VRC01-class bnAbs.

Combining data from the 15 donors analyzed individually, the overall frequency of recovered VRC01-class precursors was 1 in 2.4 million naïve B cells (Fig 2J), consistent with both our first pooled sort and a previous bioinformatically estimated range (17). The observed counts were consistent with a Poisson distribution with constant frequency of 1 in 2.4 million (Fig. 2K and (11)), suggesting that VRC01-class precursors occur at a consistent rate among 96% of humans possessing the necessary VH1-2 alleles (9). Adults have an

estimated 10^{10}–10^{11} B cells, and lymph nodes each have ~50 million B cells, of which ~65–75% are naïve B cells (19). Thus, our results indicate that VRC01-class precursor B cells are relatively common in humans: at least 2,700 to 31,000 eOD-GT8-reactive VRC01-class naïve B cells are likely present in nearly all potential human vaccinees, with ~15 such B cells in each lymph node, at any given time (20).

The K_Ds of 24 isolated VRC01-class precursors for monovalent eOD-GT8 ranged from 57 μM to 125 nM, with a geometric mean K_D of 3.4 μM (Fig. 2L and table S4), 590-fold weaker than germline-reverted VRC01-class Abs (geometric mean K_D = 5.8 nM for the panel), most likely due to the naïve CDR3 loops in the former as opposed to the affinity-matured CDR3 loops on the latter. The VRC01-class naïve B cell affinities are in the range expected to allow a multivalent eOD-GT8 immunogen, such as eOD-GT8 60mer (2, 9), to activate B cells and initiate germinal centers (21, 22). Our data also suggest that eOD-GT8 has promise to produce VRC01-class memory even given competition from non-VRC01-class B cells, as eOD-GT8 exhibited a high degree of CD4bs immunofocusing (Fig 2C), and VRC01-class precursors had an affinity advantage (≥3-fold) over non-VRC01-class CD4bs epitope-binding precursors (Fig. 2L). The frequencies and eOD-GT8 affinities of *bona fide* VRC01-class precursors isolated here warrant human immunization studies with eOD-GT8 60mer nanoparticles.

Only 2 of 20 tested VRC01-class precursors had detectable affinity for eOD-GT6 (Fig. 2L). Equilibrium binding K_Ds were 36 μM and 69 μM, and these Abs had two of the highest affinities for eOD-GT8 at 506 nM and 258 nM, respectively (table S4). These data, combined with the failure of eOD-GT6 probe B cell screens to isolate VRC01-class precursors, suggest that the engineered breadth and affinity improvements in eOD-GT8 represent a major advance toward practical utility in human vaccination.

We sought to confirm that the isolated VRC01-class precursors engage the CD4bs in the same structural binding mode as VRC01-class bnAbs (6, 17, 23–25) and germline-reverted VRC01 (9). We solved the crystal structure of isolated precursor VRC01c-HuGL2 (eOD-GT8 affinity = 368 nM) in complex with eOD-GT8 in two crystal forms (I222, 2.16 Å and C2, 2.44 Å, table S5). Comparison of this structure with the complex of core-gp120 bound to VRC01 (PDB ID: 3NGB (6)) shows the same binding mode (Fig. 3A), including specific H-CDR2 and L-CDR3 conformations (Fig. 3B) (26) that together account for over 67.2% of the Fv domain buried surface area (Fig. 3C and table S6). When interface residues of eOD-GT8 and core-gp120 are aligned, V_H and V_L of VRC01c-HuGL2 and VRC01 have high similarity (Cα RMSD 0.7 Å, Fig. 3A and fig. S9). These structural observations confirm VRC01c-HuGL2 as a *bona fide* VRC01-class precursor and support the conclusion that all of the eOD-GT8-specific naïve B cells using VH1-2 and a 5-aa L-CDR3 are *bona fide* VRC01-class precursors. Comparison of the eOD-GT8/VRC01c-HuGL2 structure with a 1.82 Å unliganded VRC01c-HuGL2 structure shows that the important H-CDR2 and L-CDR3 loops are pre-configured in the unbound state and do not require any conformational changes for engagement with gp120 CD4bs (Fig. 3D), heightening the appeal of VRC01-class germline-targeting. A 2.9 Å unliganded structure of eOD-GT8 (Fig. 3E and fig. S10) demonstrates mimicry of the VRC01-class antibody-bound conformation (27), thus helping to explain the increased affinity of eOD-GT8 for true VRC01-class bnAb precursors.

The interaction of the naïve human B cell repertoire with vaccine antigens has not been characterized previously. Given the vast immunoglobulin sequence space, direct probing of the human naïve B cell repertoire was a critical test of the physiologically relevant binding potential of the germline-targeting immunogen. The antibody sequence features, binding affinities, and high structural similarity of the eOD-GT8-specific naïve B cell-derived antibodies to VRC01 all demonstrate the power of germline-targeting design when combined with human B cell probing. Similar methods, including both protein design and human B cell probing methods, could be employed to improve and evaluate germline-targeting immunogens for other classes of HIV bnAbs and for Abs against other pathogens. These methods may be particularly important to develop and test germline-targeting approaches for bnAbs that rely heavily on HCDR3 and hence may have lower precursor frequencies.

Supplementary Material

Refer to Web version on PubMed Central for supplementary material.

Acknowledgments

We thank L. Stamatatos, T. Whitehead and M. Nussenzweig for discussions, the Flow Cytometry Core at the La Jolla Institute for Allergy and Immunology and L. Nosworthy for expert cell sorting assistance, H. Tien for technical support with crystallization robots and A. Irimia for discussions and technical help. This work was supported by the International AIDS Vaccine Initiative Neutralizing Antibody Consortium and Center (W.R.S., I.A.W., D.R.B.), CAVD funding for the IAVI NAC Center (W.R.S., I.A.W., D.R.B.), CAVD VISC (A.C.D.), the Ragon Institute of MGH, MIT and Harvard (D.R.B. and W.R.S.), the Bayer Science and Education Foundation (F.S.), the Helen Hay Whitney Foundation and Howard Hughes Medical Institute (J.G.J.), and National Institute of Allergy and Infectious Diseases grants: P01 AI094419 (W.R.S.), CHAVI-ID 1UM1AI100663 (W.R.S., S.C., I.A.W., D.R.B.), P01 AI110657 (I.A.W.), and R01 AI084817 (I.A.W.). Portions of this research were carried out at the Stanford Synchrotron Radiation Lightsource, a Directorate of SLAC National Accelerator Laboratory and an Office of Science User Facility operated for the U.S. Department of Energy Office of Science by Stanford University. The SSRL Structural Molecular Biology Program is supported by the DOE Office of Biological and Environmental Research, and by the National Institutes of Health, National Institute of General Medical Sciences (including P41GM103393). The data presented in this manuscript are tabulated in the main paper and in the supplementary materials. Coordinates and structure factors for VRC01c-HuGL2 Fab, VRC01c-HuGL2+eOD-GT8 (2.44 Å), and VRC01c-HuGL2+eOD-GT8 (2.16 Å) have been deposited with the Protein Data Bank with the accession codes 5IFA, 5IF0 and 5IES, respectively.. Sequences for heavy and light chains of HuGL1-HuGL27 have been deposited at NCBI with GenBank accession codes KU760929-KU760982. Materials and information will be provided under an MTA.

References and Notes

1. Burton DR, Mascola JR. Antibody responses to envelope glycoproteins in HIV-1 infection. Nat Immunol. 2015; 16:571–576. [PubMed: 25988889]
2. Jardine JG, et al. Priming a broadly neutralizing antibody response to HIV-1 using a germline-targeting immunogen. Science. 2015; 349:156–161. [PubMed: 26089355]
3. Dosenovic P, et al. Immunization for HIV-1 Broadly Neutralizing Antibodies in Human Ig Knockin Mice. Cell. 2015; 161:1505–1515. [PubMed: 26091035]
4. Liao HX, et al. Co-evolution of a broadly neutralizing HIV-1 antibody and founder virus. Nature. 2013; 496:469–476. [PubMed: 23552890]
5. Doria-Rose NA, et al. Developmental pathway for potent V1V2-directed HIV-neutralizing antibodies. Nature. 2014; 509:55–62. [PubMed: 24590074]
6. Zhou T, et al. Structural basis for broad and potent neutralization of HIV-1 by antibody VRC01. Science. 2010; 329:811–817. [PubMed: 20616231]

7. Scheid JF, et al. Sequence and structural convergence of broad and potent HIV antibodies that mimic CD4 binding. Science. 2011; 333:1633–1637. [PubMed: 21764753]

8. Hoot S, et al. Recombinant HIV envelope proteins fail to engage germline versions of anti-CD4bs bNAbs. PLoS pathogens. 2013; 9:e1003106. [PubMed: 23300456]

9. Jardine J, et al. Rational HIV immunogen design to target specific germline B cell receptors. Science. 2013; 340:711–716. [PubMed: 23539181]

10. McGuire AT, et al. Engineering HIV envelope protein to activate germline B cell receptors of broadly neutralizing anti-CD4 binding site antibodies. The Journal of experimental medicine. 2013; 210:655–663. [PubMed: 23530120]

11.
Materials and methods are available as supplementary materials at the Science website.

12. Whitehead TA, et al. Optimization of affinity, specificity and function of designed influenza inhibitors using deep sequencing. Nature biotechnology. 2012; 30:543–548.

13.
Filtering was done to limit library size, to exclude mutations detrimental to binding the majority of mature bnAbs, to reduce hydrophobic exposure, to exclude unpaired cysteines, and to minimize non-conservative changes to epitope components.

14. West AP Jr, Diskin R, Nussenzweig MC, Bjorkman PJ. Structural basis for germ-line gene usage of a potent class of antibodies targeting the CD4-binding site of HIV-1 gp120. Proceedings of the National Academy of Sciences of the United States of America. 2012; 109:E2083–2090. [PubMed: 22745174]

15.
Several design features of eOD-GT8 are likely responsible for this immunofocusing, including the relatively small size of eOD-GT8 (175 aa) and its compact structure (no exposed loops except Loop D and V5 within the CD4bs), as well as the glycan shielding by ten glycans covering much of the eOD-GT8 surface outside the CD4bs.

16. DeKosky BJ, et al. In-depth determination and analysis of the human paired heavy- and light-chain antibody repertoire. Nature medicine. 2015; 21:86–91.

17. Zhou T, et al. Multidonor analysis reveals structural elements, genetic determinants, and maturation pathway for HIV-1 neutralization by VRC01-class antibodies. Immunity. 2013; 39:245–258. [PubMed: 23911655]

18.
Two of the isolated VRC01-class precursors had incomplete H-CDR3 sequences preventing determination of H-CDR3 length.

19. Morbach H, Eichhorn EM, Liese JG, Girschick HJ. Reference values for B cell subpopulations from infancy to adulthood. Clin Exp Immunol. 2010; 162:271–279. [PubMed: 20854328]

20.
The frequency of 1 in 2.4 million is an underestimate of the true frequency among naïve B cells, because not all B cells counted by the sorter as eOD-GT8$^{tri+/SA+}$/eOD-GT8-KO^{-} were sorted into a well (cell sorter loss), paired heavy chain and light chain (HC and LC) sequences were recovered from fewer than half of eOD-GT8$^{tri+/SA+}$/eOD-GT8-KO^{-} B cells sorted into wells [a result of the inherent limitations of single-cell polymerase chain reaction (PCR)], and B cells bearing lambda light chains were not analyzed. By correcting for cell sorter and PCR losses, the frequency of VRC01-class naïve B cell precursors is calculated as 1 in 400,000 naïve B cells (11). VRC01-class precursors may also exist in the memory B cell population in healthy humans, but their frequency remains to be measured.

21. Shih TA, Meffre E, Roederer M, Nussenzweig MC. Role of BCR affinity in T cell dependent antibody responses in vivo. Nat Immunol. 2002; 3:570–575. [PubMed: 12021782]

22. Dal Porto JM, Haberman AM, Kelsoe G, Shlomchik MJ. Very low affinity B cells form germinal centers, become memory B cells, and participate in secondary immune responses when higher affinity competition is reduced. The Journal of experimental medicine. 2002; 195:1215–1221. [PubMed: 11994427]
23. Wu X, et al. Focused evolution of HIV-1 neutralizing antibodies revealed by structures and deep sequencing. Science. 2011; 333:1593–1602. [PubMed: 21835983]
24. Diskin R, et al. Increasing the potency and breadth of an HIV antibody by using structure-based rational design. Science. 2011; 334:1289–1293. [PubMed: 22033520]
25. Diskin R, et al. Restricting HIV-1 pathways for escape using rationally designed anti-HIV-1 antibodies. The Journal of experimental medicine. 2013; 210:1235–1249. [PubMed: 23712429]
26. Zhou T, et al. Structural Repertoire of HIV-1-Neutralizing Antibodies Targeting the CD4 Supersite in 14 Donors. Cell. 2015; 161:1280–1292. [PubMed: 26004070]
27.
We conclude that mutations that led to the design of eOD-GT8 from eOD-GT6 further stabilize the antibody-bound state, based on a higher similarity between the VRC01c-HuGL2-bound and unliganded eOD-GT8 (all-atom rmsd= 0.98 Å, alignment of 1206 atoms) vs GL-VRC01-bound (PDBID: 4JPK) and unliganded (PDBID: 4JPJ) eOD-GT6 (all-atom rmsd= 3.0 Å, alignment of 1343 atoms) (fig. S10).
28. Kwakkenbos MJ, et al. Generation of stable monoclonal antibody-producing B cell receptor-positive human memory B cells by genetic programming. Nature medicine. 2010; 16:123–128.
29. Tiller T, et al. Efficient generation of monoclonal antibodies from single human B cells by single cell RT-PCR and expression vector cloning. J Immunol Methods. 2008; 329:112–124. [PubMed: 17996249]
30. Kabsch W. Xds. Acta Crystallogr D Biol Crystallogr. 2010; 66:125–132. [PubMed: 20124692]
31. Strong M, et al. Toward the structural genomics of complexes: crystal structure of a PE/PPE protein complex from Mycobacterium tuberculosis. Proceedings of the National Academy of Sciences of the United States of America. 2006; 103:8060–8065. [PubMed: 16690741]
32. McCoy AJ, et al. Phaser crystallographic software. J Appl Crystallogr. 2007; 40:658–674. [PubMed: 19461840]
33. Adams PD, et al. PHENIX: a comprehensive Python-based system for macromolecular structure solution. Acta Crystallogr D Biol Crystallogr. 2010; 66:213–221. [PubMed: 20124702]
34. Emsley P, Cowtan K. Coot: model-building tools for molecular graphics. Acta Crystallogr D Biol Crystallogr. 2004; 60:2126–2132. [PubMed: 15572765]
35. Heinig M, Frishman D. STRIDE: a web server for secondary structure assignment from known atomic coordinates of proteins. Nucleic Acids Res. 2004; 32:W500–502. [PubMed: 15215436]
36. Chen VB, et al. MolProbity: all-atom structure validation for macromolecular crystallography. Acta Crystallogr D Biol Crystallogr. 2010; 66:12–21. [PubMed: 20057044]
37. Otwinowski Z, Minor W. Processing of x-ray diffraction data collected in oscillation mode. Methods in Enzymology. 1997; 276:307–326.
38. Krissinel E, Henrick K. Inference of macromolecular assemblies from crystalline state. J Mol Biol. 2007; 372:774–797. [PubMed: 17681537]
39. Wu X, et al. Rational design of envelope identifies broadly neutralizing human monoclonal antibodies to HIV-1. Science. 2010; 329:856–861. [PubMed: 20616233]
40. Li Y, et al. HIV-1 neutralizing antibodies display dual recognition of the primary and coreceptor binding sites and preferential binding to fully cleaved envelope glycoproteins. Journal of virology. 2012; 86:11231–11241. [PubMed: 22875963]
41. Georgiev IS, et al. Delineating antibody recognition in polyclonal sera from patterns of HIV-1 isolate neutralization. Science. 2013; 340:751–756. [PubMed: 23661761]

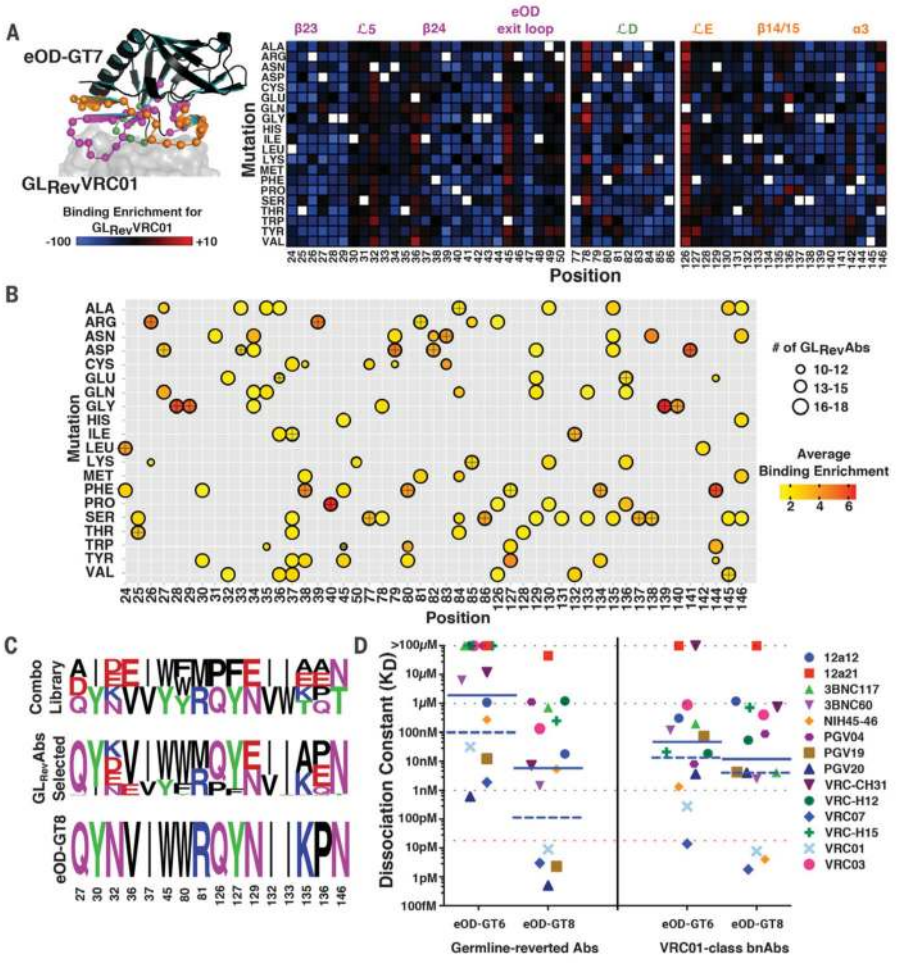

Fig. 1. Development of eOD-GT8

(**A**) Model of germline-reverted VRC01 (gray surface) interacting with eOD-GT7 (cartoon) with the 58 positions subjected to deep mutational scanning shown as magenta, green and orange spheres representing the three mutagenized linear segments. Binding enrichments, the ratio of the frequency of a mutation in the top 10% binding population to the frequency of the same mutation in all cells displaying eOD-GT7, were computed for each mutation on eOD-GT7 for germline-reverted VRC01 and are shown as a heatmap on the right, in which blue indicates unfavorable mutations, red indicates favorable mutations and white indicates the amino-acid residue in eOD-GT7. (**B**) The combined binding enrichments from independent yeast display screens for 18 germline-reverted VRC01-class bnAbs are shown as a multi-dimensional heatmap in which the color scale from yellow to red indicates increasing favorable average enrichment and the symbol sizes reflect the breadth of enrichment, the number of germline-reverted Abs with enriched binding for each point mutation. If enriched, the eOD-GT7 amino-acid residue is indicated by crosses. (**C**) Sequence logos depicting amino acids at each of 16 positions in the combinatorial library (top), the sequences selected from the combinatorial library for improved binding to germline-reverted VRC01-class bnAbs (middle), and the final sequence of eOD-GT8 (bottom). (**D**) SPR dissociation constants measured for both germline-reverted and mature

VRC01-class bnAbs against eOD-GT6 and eOD-GT8. Solid blue lines show geometric mean measured over all the data, using the value K_D = 100 μM for samples with K_D > 100 uM; dashed blue lines show geometric means computed for the 8 germline-reverted Abs or 12 bnAbs for which K_Ds < 100 μM could be measured for both eOD-GT6 and eOD-GT8. The red dotted line signifies the limit of detection for our SPR instrument (16 pM); K_Ds below this value were measured by KinExa.

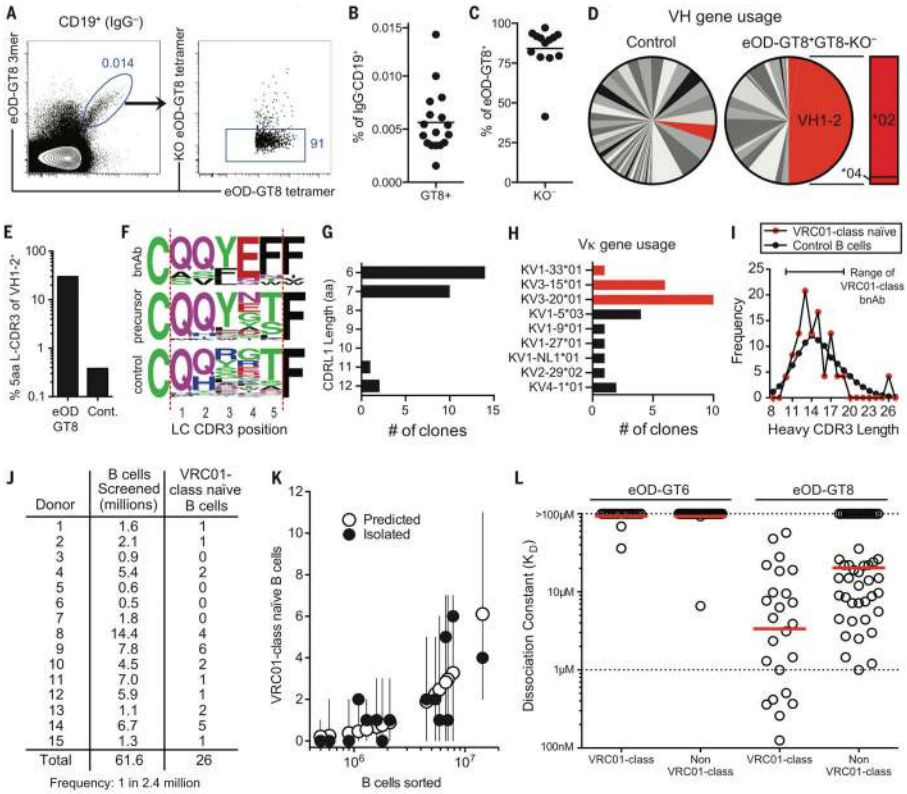

Fig. 2. eOD-GT8-binding VRC01-class naïve B cells exist in healthy human donors

(**A**) eOD-GT8^{+} naïve CD19^{+}IgG^{-} B cells. (**B**) eOD-GT8^{+} B cell frequency (**C**) and eOD-GT8 KO$^{(-)}$ cells among eOD-GT8^{+} B cells in individual donors. (**D**) VH1-2 usage among eOD-GT8^{+}/eOD-GT8 KO$^{(-)}$ sorted B cells (n=173) versus control B cells. VH1-2 (red) allele frequencies are indicated. **(E)** B cells expressing a 5-aa L-CDR3 among VH1-2^{+} B cells isolated by eOD-GT8 versus control B cells. **(F)** L-CDR3 sequence logos of VRC01-class bnAbs (top), VRC01-class naïve precursors (middle), and control B cells (bottom). **(G)** L-CDR1 lengths of 27 VRC01-class naïve B cells. (**H**) Light chain V gene usage of 27 VRC01-class naïve B cells. Known VRC01-class bnAb Vκ are red. (**I**) H-CDR3 lengths of VRC01-class naïve B cells versus control B cells. (**J**) Total B cells screened and VRC01-class naïve B cells found in 15 individuals. (**K**) Poisson distribution modeling of the number of VRC01-class naïve B cells. Vertical lines show the 2.5% and 97.5% quantiles. (**L**) SPR dissociation constants for eOD-GT6 or eOD-GT8 binding to VRC01-class or non-VRC01-class Abs derived from eOD-GT8-sorted human naïve B cells. Solid red lines indicate geometric mean.

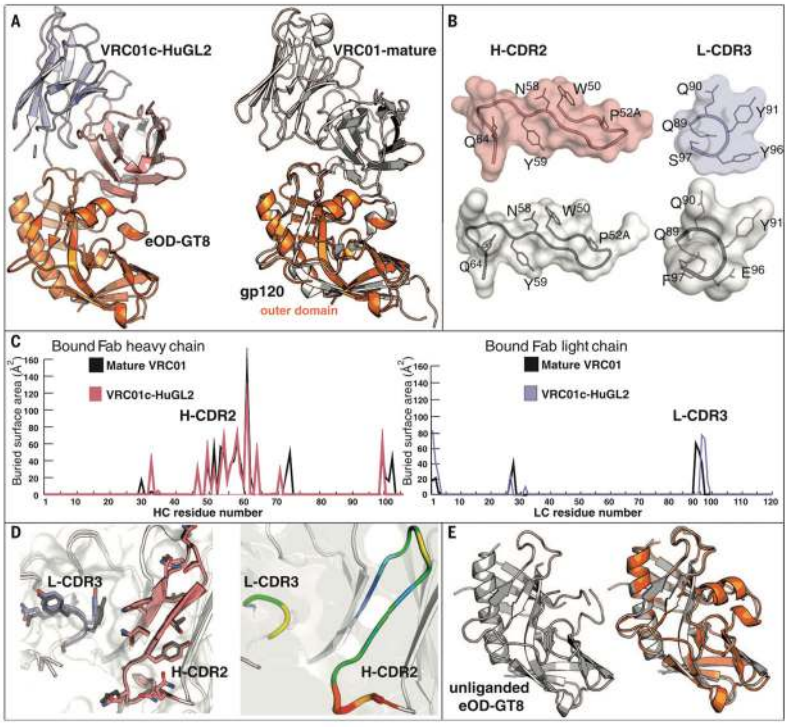

Fig. 3. Structural analysis of eOD-GT8 and human germline antibody VRC01c-HuGL2 complex

(**A**) Crystal structures of VRC01c-HuGL2+eOD-GT8 (LC: blue, HC: salmon and eOD-GT8: orange) and of mature VRC01+gp120 (PDB ID: 3NGB in white) shown in the same orientation, showing eOD-GT8 superimposed on gp120, and showing only the antibody Fv regions for clarity. (B) Comparison of the H-CDR2 and L-CDR3 conformations from the structures in (A). (C) Comparison of buried surface areas for the V_H and V_L residues of VRC01c-HuGL2 and mature VRC01+gp120, in their bound forms. (D) Comparison of H-CDR2 and L-CDR3 conformations of unliganded and eOD-GT8-liganded VRC01c-HuGL2 Fab. All atoms of V_H and V_L were aligned. In the left image, H-CDR2 and L-CDR3 are shown as sticks; in the right image the CDRs are shown according to B-factors reporting local structural flexibility using a relative scale in which increasing wire thickness and warmness of color (blue to red) indicates increasing mobility. (E) Crystal structure of unliganded eOD-GT8 shown in cartoon and surface (left) and a superposition of unliganded and VRC01c-HuGL2-bound forms of eOD-GT8 (right; Cα RMSD = 0.4 Å).